Supplementary Material

Modelling porcine reproductive and respiratory syndrome virus dissemination dynamics to quantify the contribution of multiple modes of transmission: between-farm pig and vehicle movements, farm-to-farm proximity, feed ingredients, and re-break

Jason A. Galvis [1], Cesar A. Corzo[2], Gustavo Machado[1]*

[1]Department of Population Health and Pathobiology, College of Veterinary Medicine, Raleigh, North Carolina, USA.

[2]Veterinary Population Medicine Department, College of Veterinary Medicine, University of Minnesota, St Paul, MN, USA.

***Corresponding author:** gmachad@ncsu.edu

Section 1. A descriptive analysis of model parameters used in the PRRSV simulated transmission.

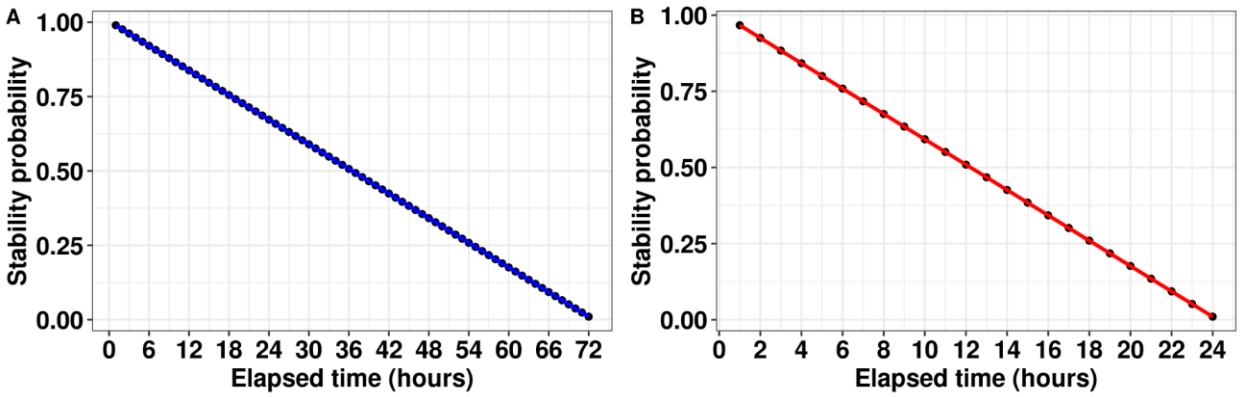

Figure S1. The distribution of PRRSV stability probability on vehicle surface over time. In A), we show the decay of cold season which included the months between October to March, and B) warm season decay in PRRSV suitability which included the months between April to September. In summary, here we assumed that PRRSV suitability decreased linearly over time, in which for cold months after 72 hours the suitability of PRRSV was set to zero, the same applied to warm weather in which at hour 24 after a vehicle visited an infected farm PRRSV was no longer viable. This approach was used for all vehicle related contact networks including vehicles transporting feed, pigs-to-farm, pigs-to-market and crew.

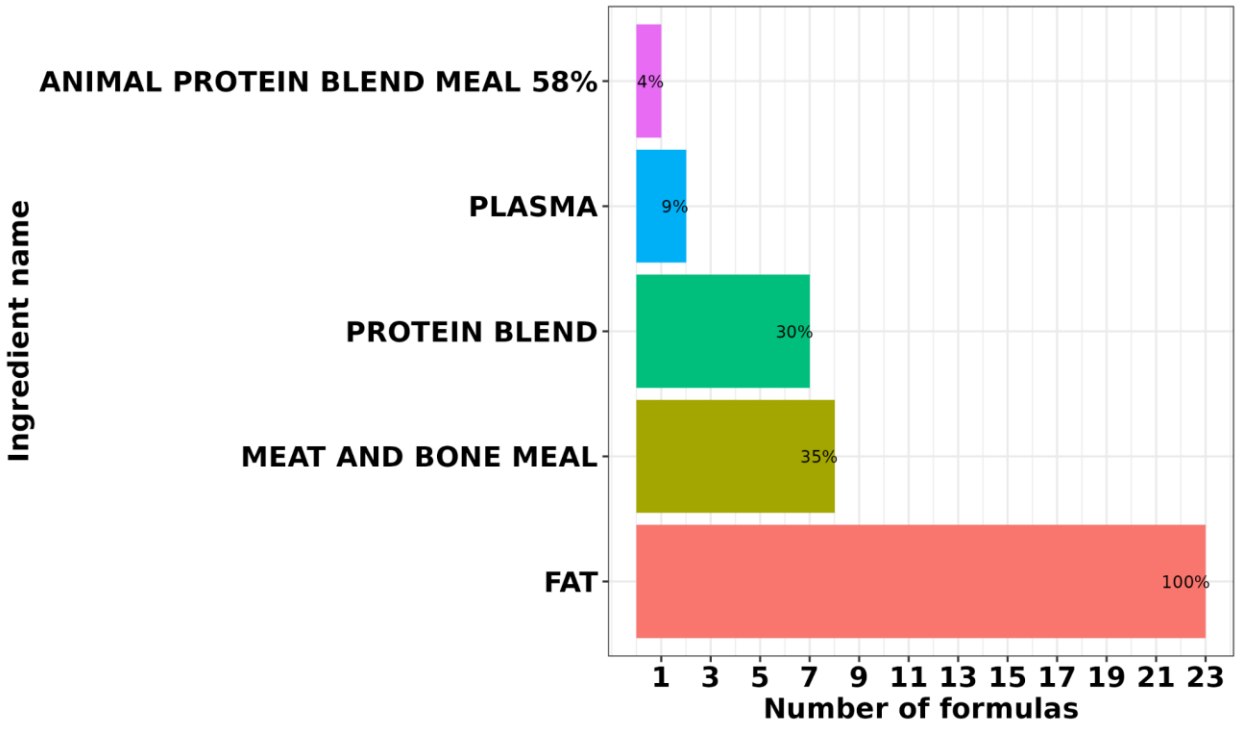

Figure S2. The overall proportion of animal by-products delivered to farms from January 2020 until December 2020. The x-axis shows the number of unique feed formulations and the y-axis each animal by-product utilized by company A.

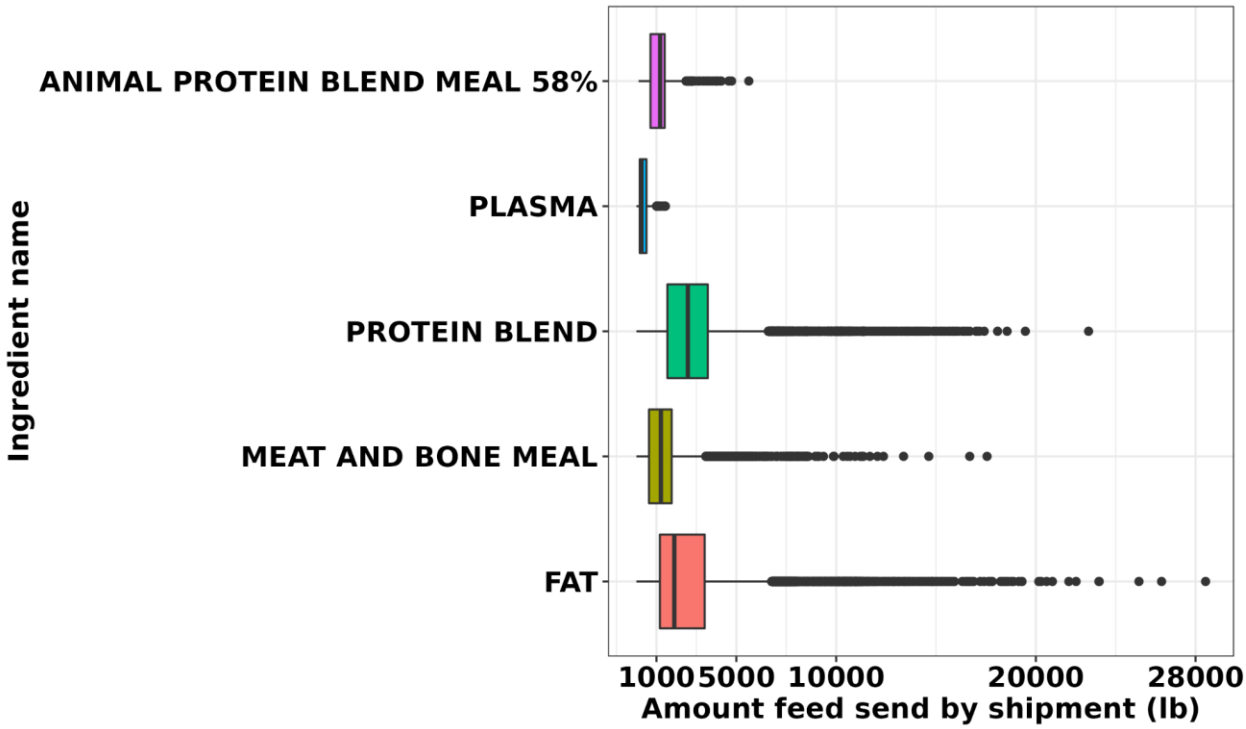

Figure S3. The weight (lb) distribution of animal by-products in shipments of feed formulation delivered to the farms in the study area over from January 2020 until December 2020.

Table S1. Terminology and definition from the social network analysis.

Network terminology	**Definition**	**Reference**
Node	Element of the network representing the farms.	-
Edge	Link among two nodes.	-
Static network	Once an edge exists between two nodes, it is present for the whole time period.	(Kao et al., 2007)
Temporal network	The edges between two nodes only exist at different time steps.	(Lentz et al., 2016)
Density	Represent the proportion of edges among nodes in the network that are actually present.	(Wasserman and Faust, 1994)
Causal fidelity	Quantify the error of the static representation of a temporal network by comparing the number of paths in the static and temporal networks.	(Lentz et al., 2016)
Strongly	It is a subset of nodes for which a *directed* path exists	(Lentz et al., 2016)

Connected Component (SCC)	between all pairs of them allowing them to be mutually accessible by following the direction of the links in the network.	
Larger Strongly Connected Component (LSCC)	It is the larger number of nodes in a strong connected component.	(Lentz et al., 2016)
In-degree	Number of nodes providing animals to a specific node.	(Wasserman and Faust, 1994)
Out-degree	Number of nodes obtaining animals from a specific node.	(Wasserman and Faust, 1994)
Betweenness	The frequency of a node is in the shortest path between pairs of other nodes in the network.	(Freeman, 1978)
Ingoing contact chain (ICC)	Subsets of nodes that can reach a specific node by direct contact or indirect contacts through a sequential order of edges through other nodes using the temporal network.	(Nöremark and Widgren, 2014)
Outgoing contact chain (OCC)	Subsets of nodes that can be reached by a specific node by direct contact or indirect contacts through a sequential order of edges through other nodes using the temporal network.	(Nöremark and Widgren, 2014)

To calculate the barrier index (vegetation level, utilized to modulate the probability of local transmission), we used a linear regression, to express PRRSV infected farms from 2020 as a function of the Enhanced Vegetation Index (EVI) and yearly seasonality (spring, summer, fall and winter). We found that PRRSV frequency decreased as EVI increased, with a stronger association in winter and fall seasons (Figure S4). Here we used the regression coefficients to predict weekly PRRSV incidence, which then were transformed into parameter *a*, which was scaled into values between [0, 1], later utilized to modulate the local transmission.

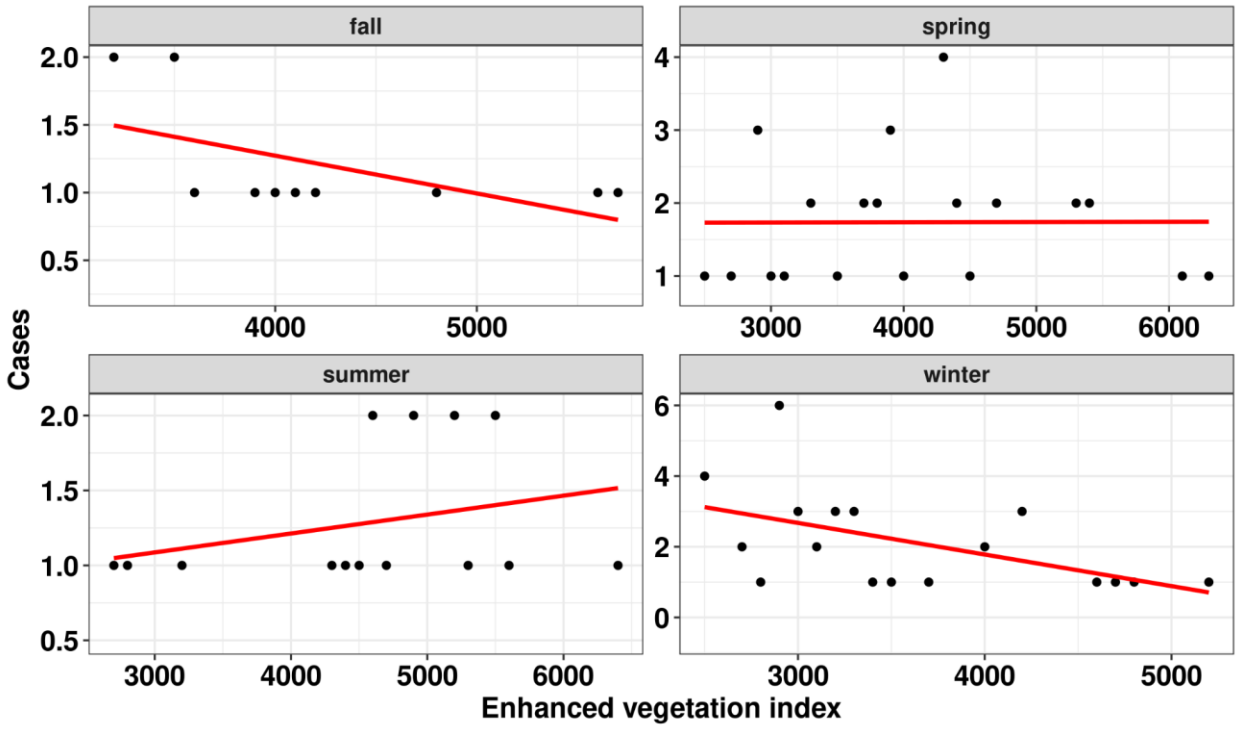

Figure S4. Linear regression of PRRSV infected farms. The y-axis is the number of PRRSV outbreaks and in the x-axis EVI.

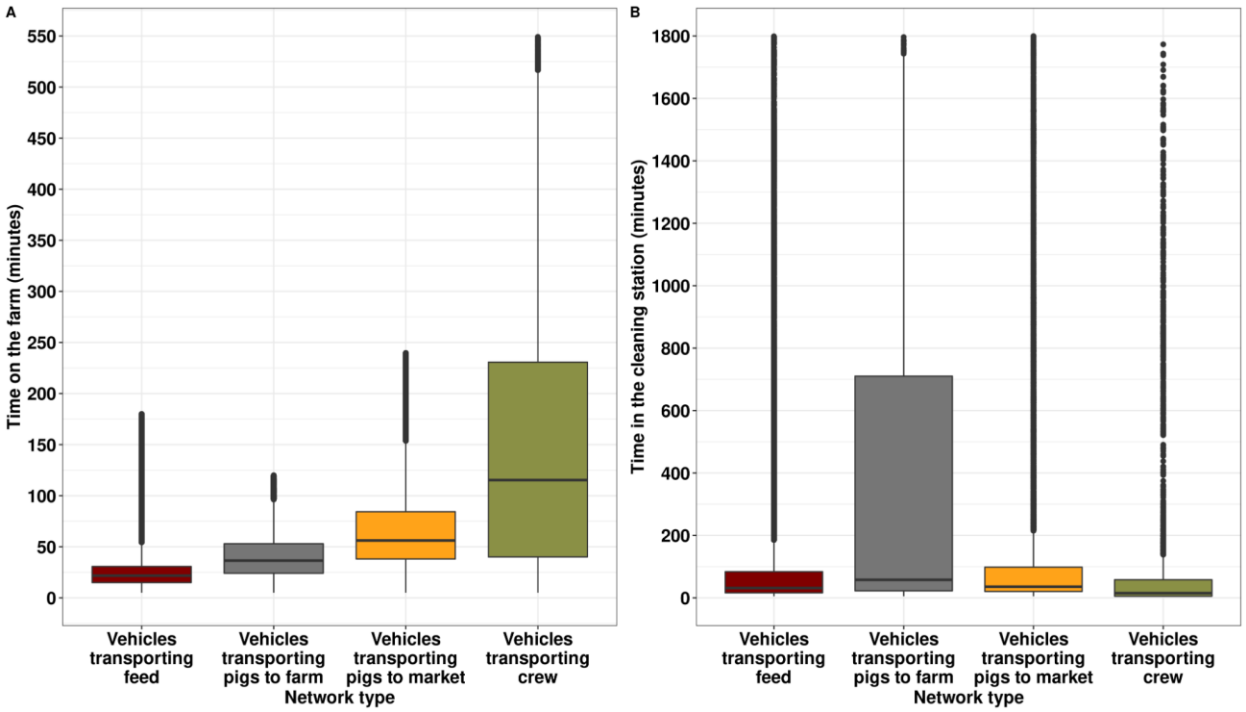

Figure S5. The time vehicles spent on each farm visit. The boxplot shows the distribution in minutes that each vehicle remained within farms premises in A) and at cleaning stations in B).

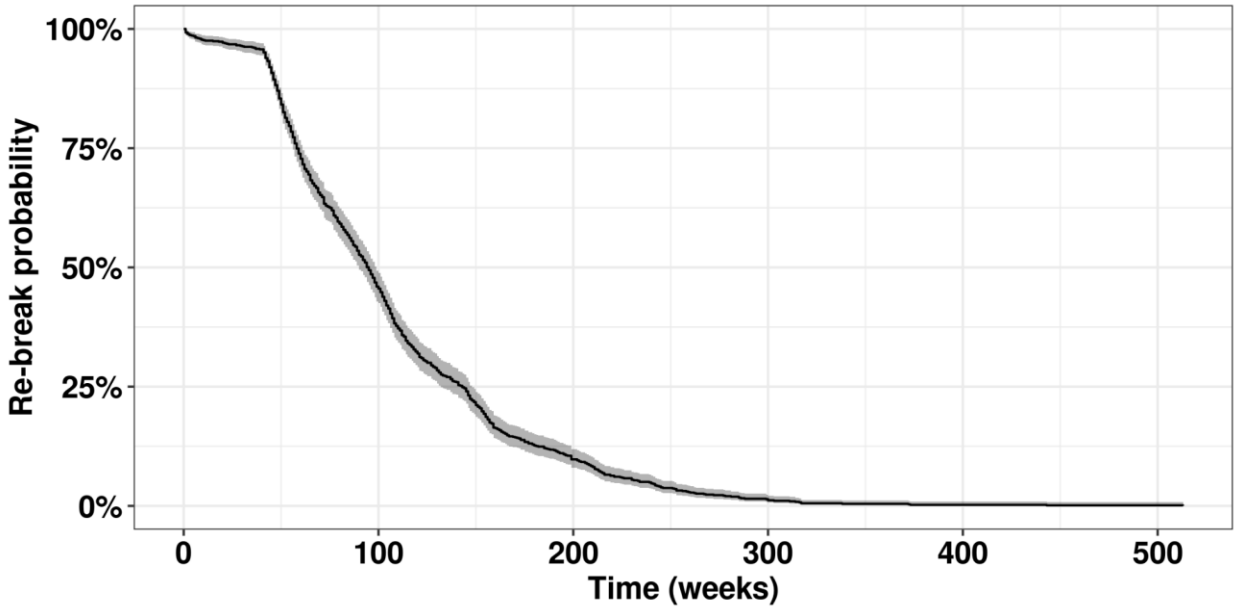

Figure S6. A survival analysis of infected and recovered farms from 2009 to 2019. In this example we shown the distribution used for each farm to calibrate the re-break probability

Figure S7. Monthly seasonality index calculated from the frequency of PRRSV, calculated by an additive moving average decomposition derived from analysis of the PRRSV records from 2015 to 2019.

Section 2: Model calibration and main model outputs

In Table S2 we show the summary statistics used in step 1 of the Approximate Bayesian Computation (ABC) rejection algorithm, where the tolerance interval represents the square error allowed from the simulation to the observed values.

Table S2. Summary statistics used by the ABC Sequential Monte Carlo rejection algorithm for the model.

Summary statistics	**Observed values**	**Tolerance interval (ϵ)**
Total number of sow farms with detected cases	96	20
The weekly average number of sow farms with detected cases	1.8	0.5
The weekly maximum number of sow farms with detected cases	9	5
Total number of nursery farms with detected cases	37	20
The weekly average number of nursery farms with detected cases	0.7	0.5
The weekly maximum number of nursery farms with detected cases	6	5
Total number of finisher farms with detected cases	17	20
The weekly average number of finisher farms with detected cases	0.3	0.5
The weekly maximum number of finisher farms with detected cases	2	5

Expected prevalence in finisher and nursery farms	30% (expert opinion)	100

To assess the model performance, we evaluated the probability to predict cells (10 x 10 km squares) with true infected cells (cells where at least one sow farm outbreak was recorded) at time *t*. Each sow farm was allocated to a cell in the spatial grid (total of 154 cells in the study area). The risk of each cell was calculated by the sum of times at least one farm within a cell was identified with infected status after 100 simulations based on the distribution of the estimated risk values; we utilized a percentiles thresholds (r) approach to determine cells at high and low risk. Where high risk cells were compared with the true infected cells at time *t*. Subsequently we estimate the model sensitivity and specificity, for all thresholds, as follows:

$$S_r = TP_r/(TP_r + FN_r)$$

$$E_r = TN_r/(TN_r+FP_r)$$

where true positives (TP) was the subset of cells with observed outbreaks and the estimated risk was above the r threshold; false negatives (FN) was the subset of cells with observed outbreaks and the estimated risk was below the r threshold; true negative (TN) was the subset of cells without observed outbreaks and the estimated risk was below the r threshold; and false positives (FP) was the subset of cells without observed outbreaks and the estimated risk above the r threshold. It is worth noting that cells with zero risk were not considered in the sensitivity analysis.

In step 2 of the ABC rejection algorithm, the sensitivity and specificity were calculated for each particle accepted in the step 1 of model fitting. The particles accepted were those with sensitivity values ≥30% with r = 85th and ≥50% with r = 70th. The priors for each parameter were drawn from a uniform distribution that ranged between 0 and 1.5 for pig movements transmission rate, 0 and 0.001 for local transmission, the four transporting vehicles and amount of fat and meat and bone in the feed meals transmission rates, and finally between 0 and 0.01 for re-break transmission rate. These range values were chosen according to model performance to fit the temporal and spatial distribution of PRRSV cases through

some test simulations, thus reducing the number of simulations and processing time in the model calibration.

Table S3. Transmission parameters used in simulations, for the distribution of the posterior parameter.

Model parameter	**Symbol**	**Average values**	**95% interval**	**Details & references**
Transmission rate of pig movements	β_n	0.428	0.36-0.49	ABC fitting
Local transmission rate	β_l	0.00055	0.0005-0.0006	ABC fitting
Transmission rate of vehicles transporting feed	β_f	0.000014	0.000012-0.000016	ABC fitting
Transmission rate of vehicles transporting pigs to farms	β_p	0.00026	0.00021-0.00030	ABC fitting
Transmission rate of vehicles transporting pigs to market	β_m	0.00049	0.00043-0.00055	ABC fitting
Transmission rate of vehicles transporting crew	β_c	0.00027	0.00023-0.00031	ABC fitting
Transmission rate of fat in the feed meal	β_a	0.00042	0.00036-0.00048	ABC fitting
Transmission rate of meat and bone in the feed meal	β_b	0.00042	0.00036-0.00048	ABC fitting
Transmission rate of	β_r	0.0045	0.004-0.005	ABC fitting

re-break				
Farm' biosecurity	H(sow)	0.57	0.51-0.63	ABC fitting
Maximum effective surveillance	L(sow)	0.95	-	Expert opinion
	L(nurseries)	0.048	0.044-0.051	ABC fitting
	L(finisher)	0.0015	0.0013-0.0017	ABC fitting
	L(others)	0.045	0.040-0.051	ABC fitting
PRRSV seasonality	T	Weekly values calculated	-	Figure S7
Average time for PRRSV detection	X0	4 weeks	-	Expert opinion
Average infectious time sow farms	-	41 weeks	-	(Sanhueza et al., 2019)

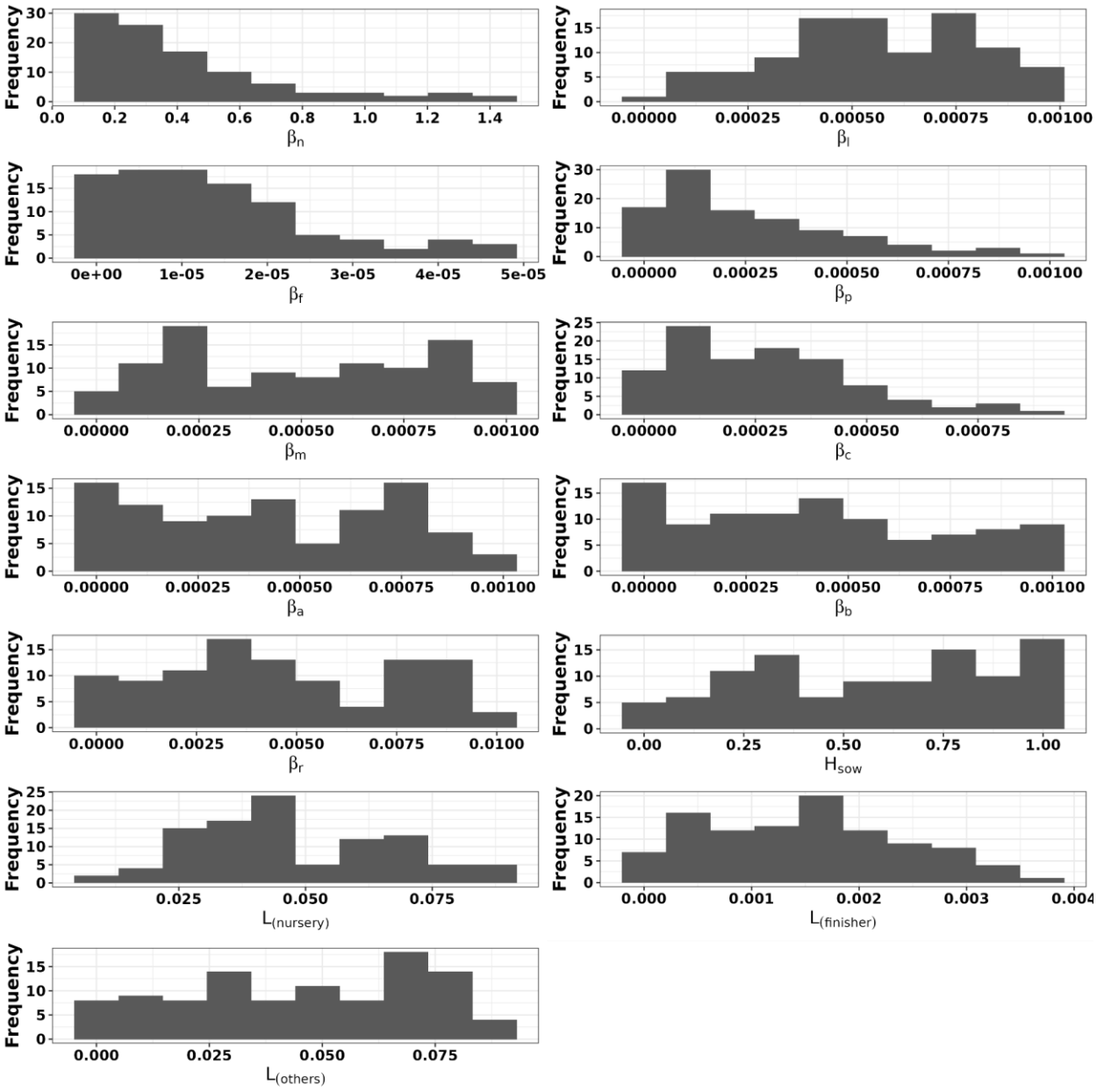

Figure S8. Posterior distribution of the calibrated transmission parameters derived from 100 accepted particles.

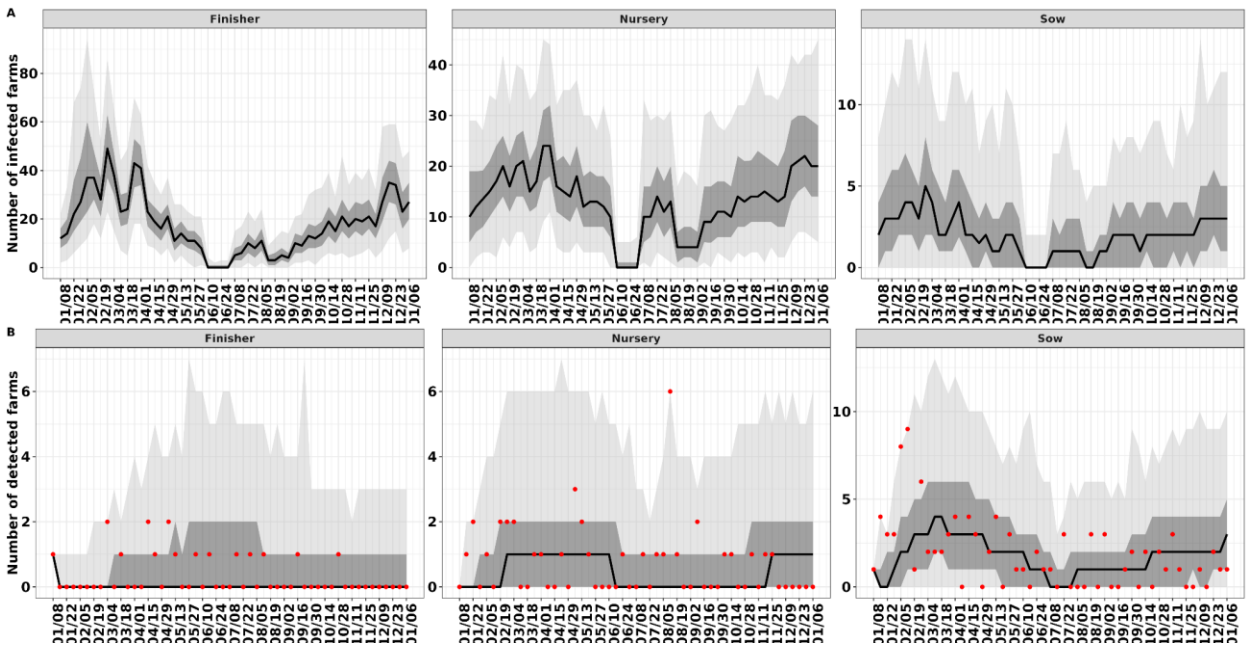

Figure S9. The simulated weekly number of infected farms in A) and infected detected farms (PRRSV outbreaks) in B). The black line represents the median, the dark shade areas represent a 75% credible interval and the light shade areas maximum and minimum generated by the model, and the red dots the frequency of true outbreaks reported in our data. Uncertainty in the estimated model parameters is reflected by 1,000 repeated simulations.

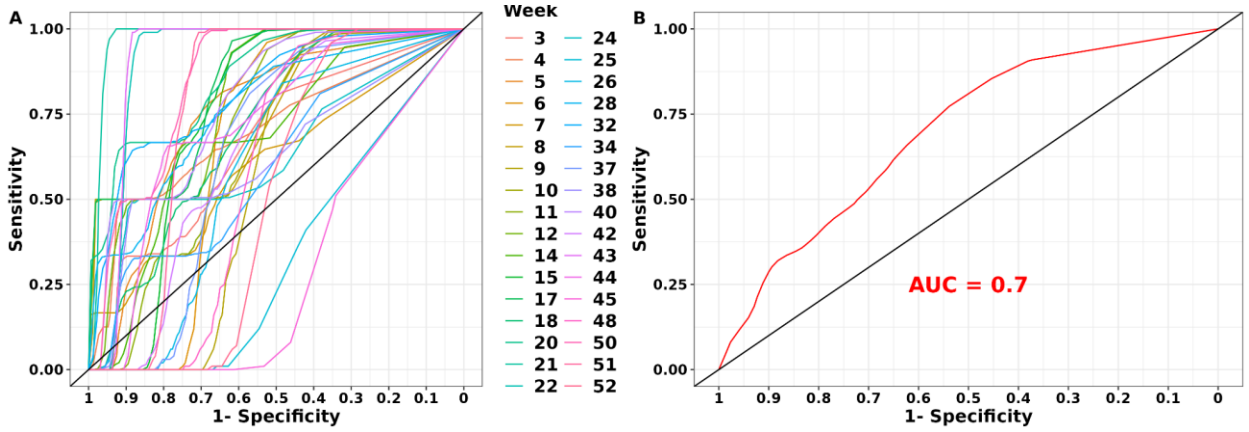

Figure S10. The average sensitivity and specificity for the weekly forecasts in A) and the average of all weeks in B) values calculated from 100 model calculations with each model calculation having 100 individual model iterations.

Section 3: Descriptive analysis of the between-farm pig movements and transportation vehicle movement networks, and the quantity of animal by-product in feed ingredients.

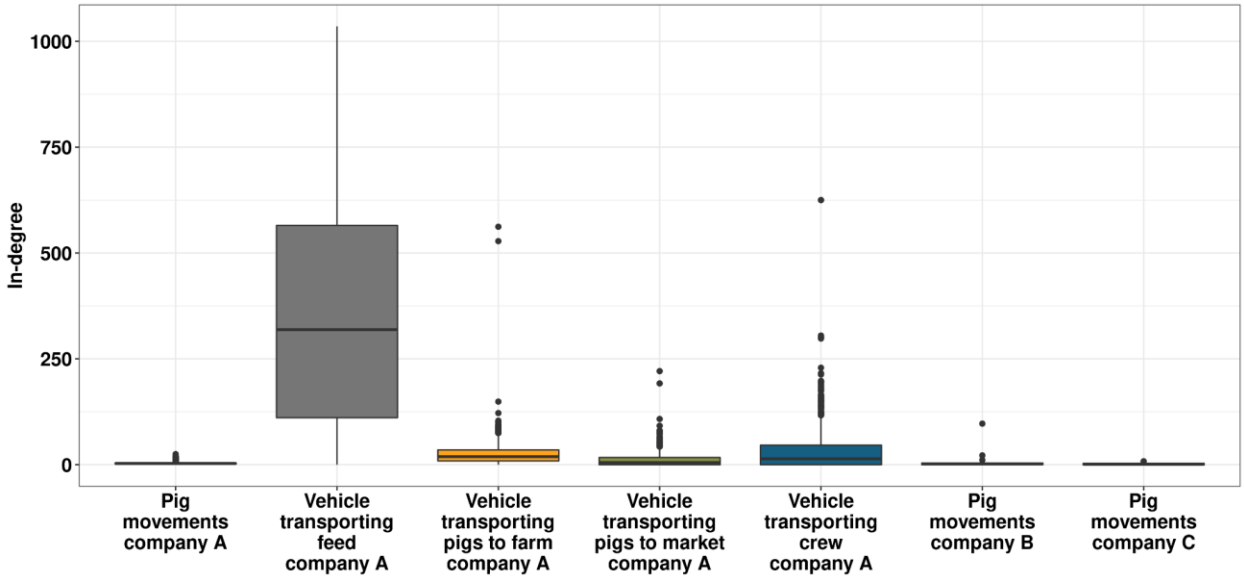

Figure S11. Boxplot with the distribution of in-degree for between-farm pig movements of each transportation vehicle movement networks.

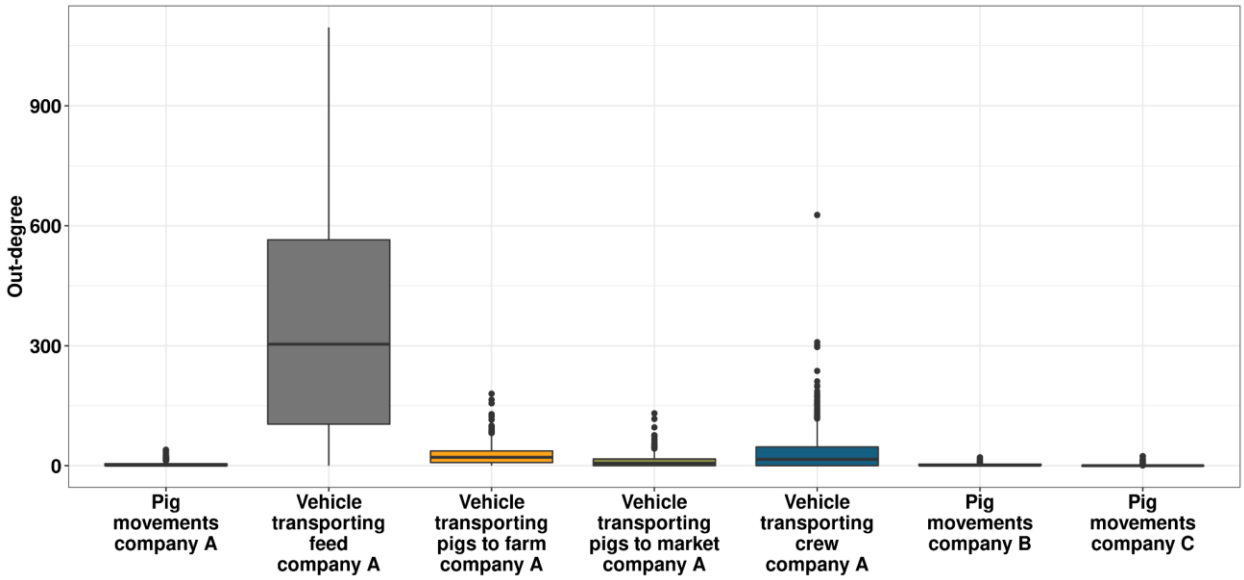

Figure S12. Boxplot with the distribution of out-degree for between-farm pig movements of each transportation vehicle movement networks.

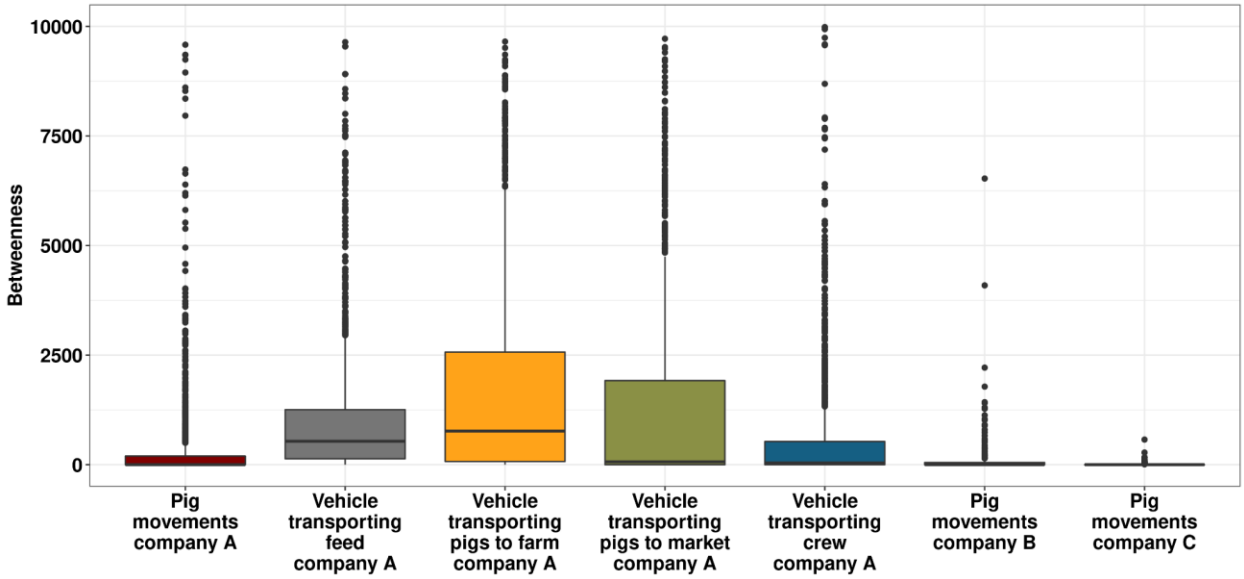

Figure S13. Boxplot with the distribution of betweenness for between-farm pig movements of each transportation vehicle movement networks.

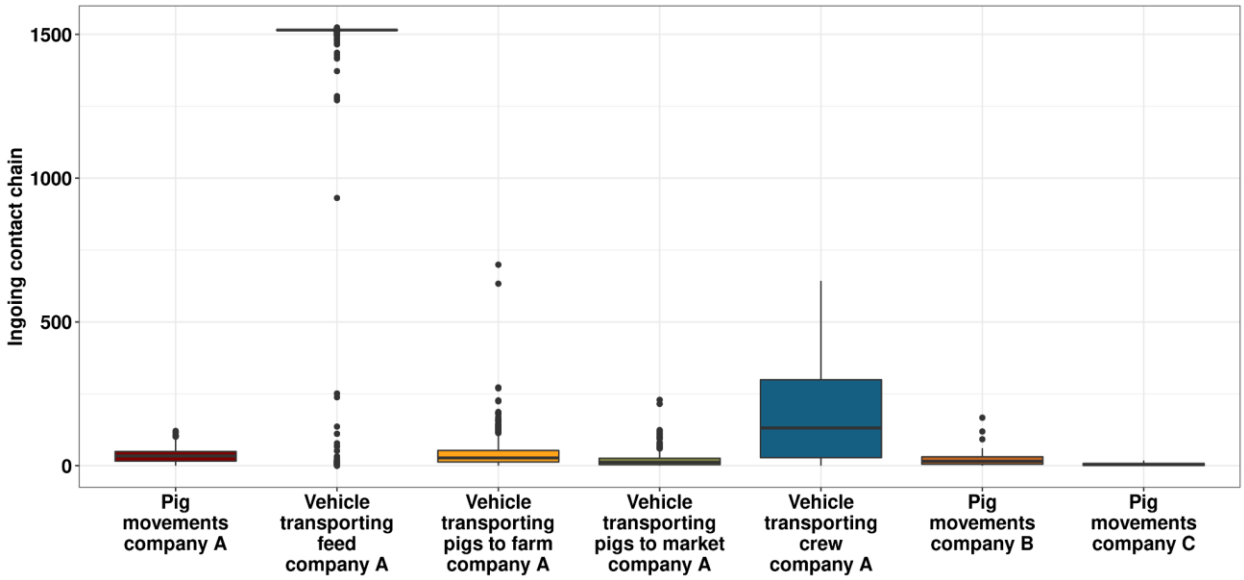

Figure S14. Boxplot with the distribution of ingoing contact chains for between-farm pig movements of each transportation vehicle movement networks.

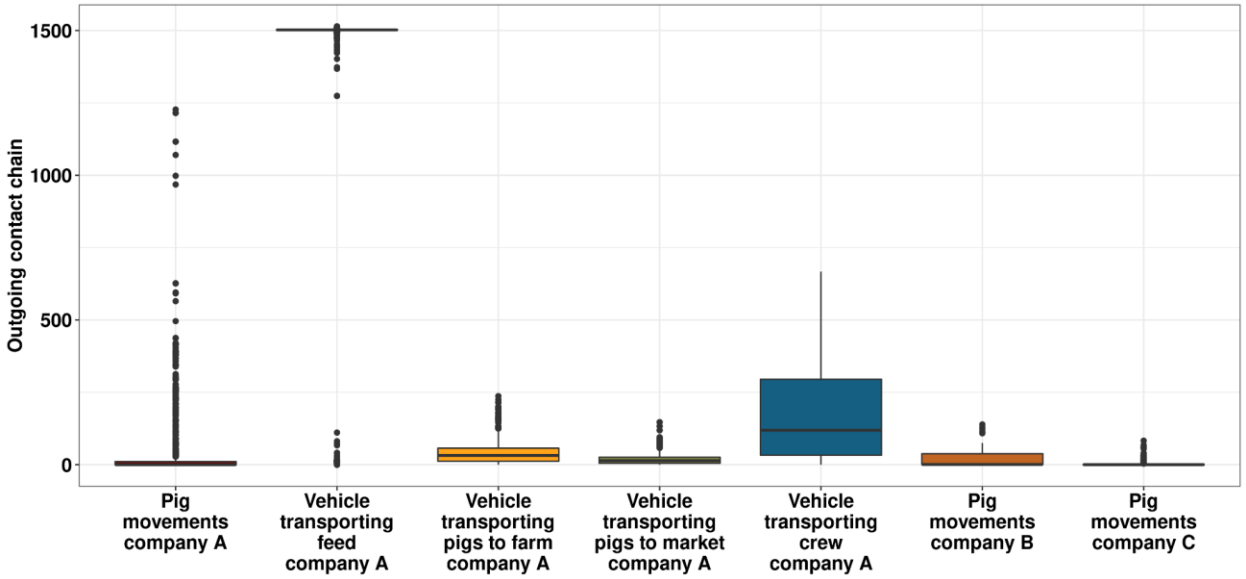

Figure S15. Boxplot with the distribution of outgoing contact chains for between-farm pig movements of each transportation vehicle movement networks.

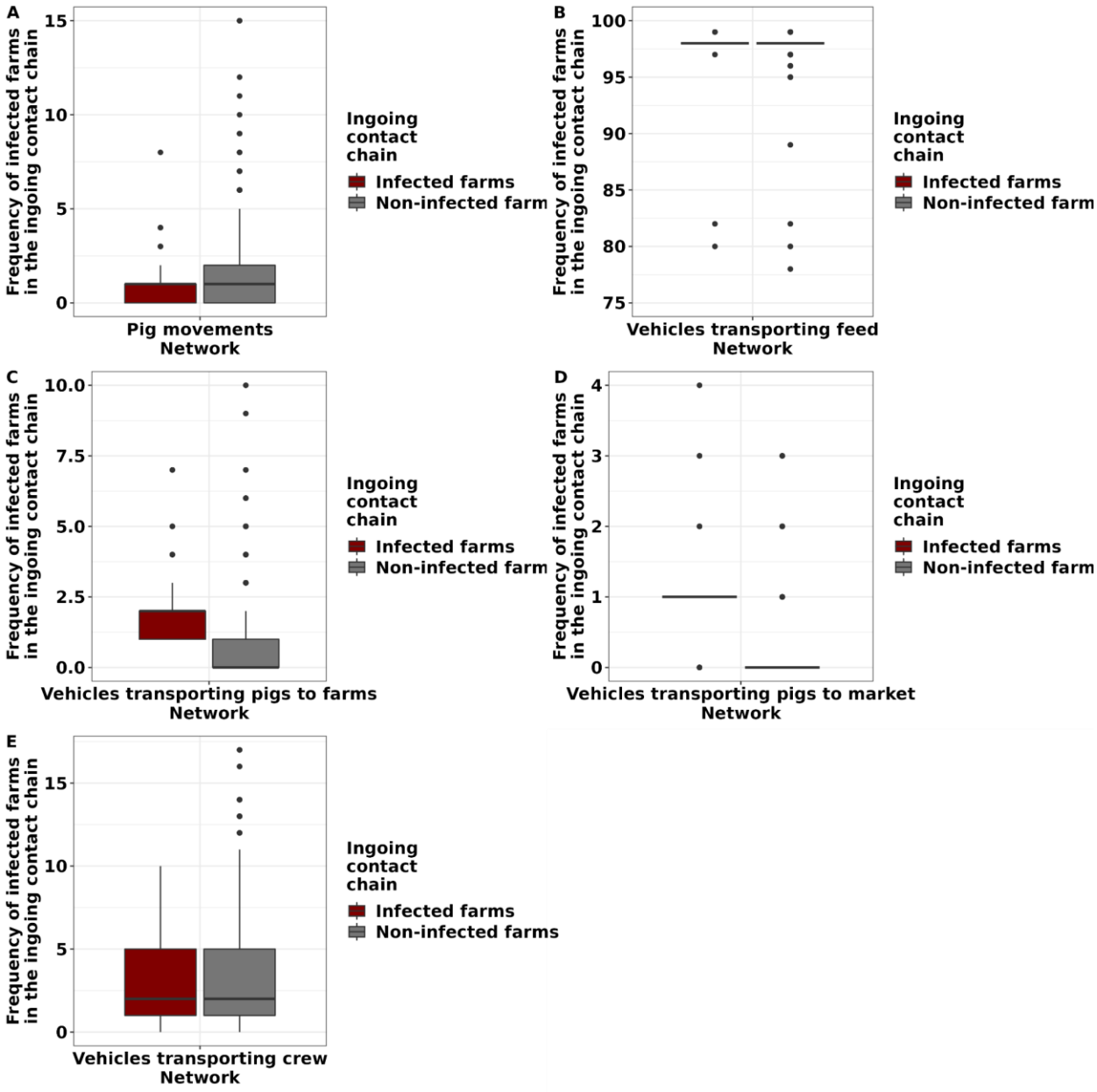

Figure S16. Boxplot comparing the frequency of infected farms in the ingoing contact chain of infected and non-infected farms of each transportation vehicle and pig movement networks. Infected farms are more frequent in the ingoing contact chain of other infected farms for the vehicles transporting feed, pigs to farms and pigs to market (Mann Whitney test $p < 0.05$).

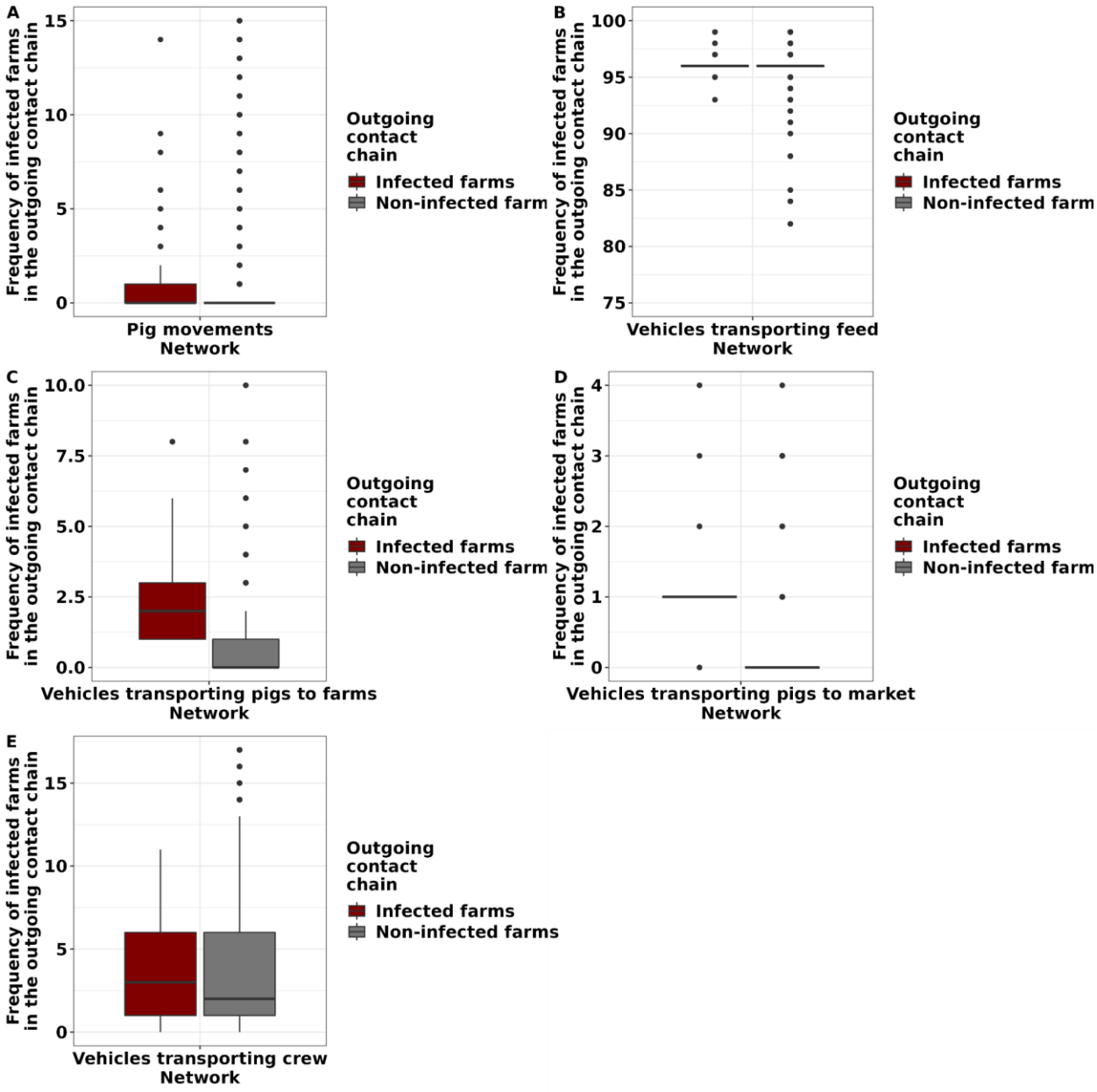

Figure S17. Boxplot comparing the frequency of infected farms in the outgoing contact chain of infected and non-infected farms of each transportation vehicle and pig movement networks. Infected farms are more frequent in the outgoing contact chain of other infected farms for pig movements and the vehicles transporting feed, pigs to farms and pigs to market (Mann Whitney test $p < 0.05$).

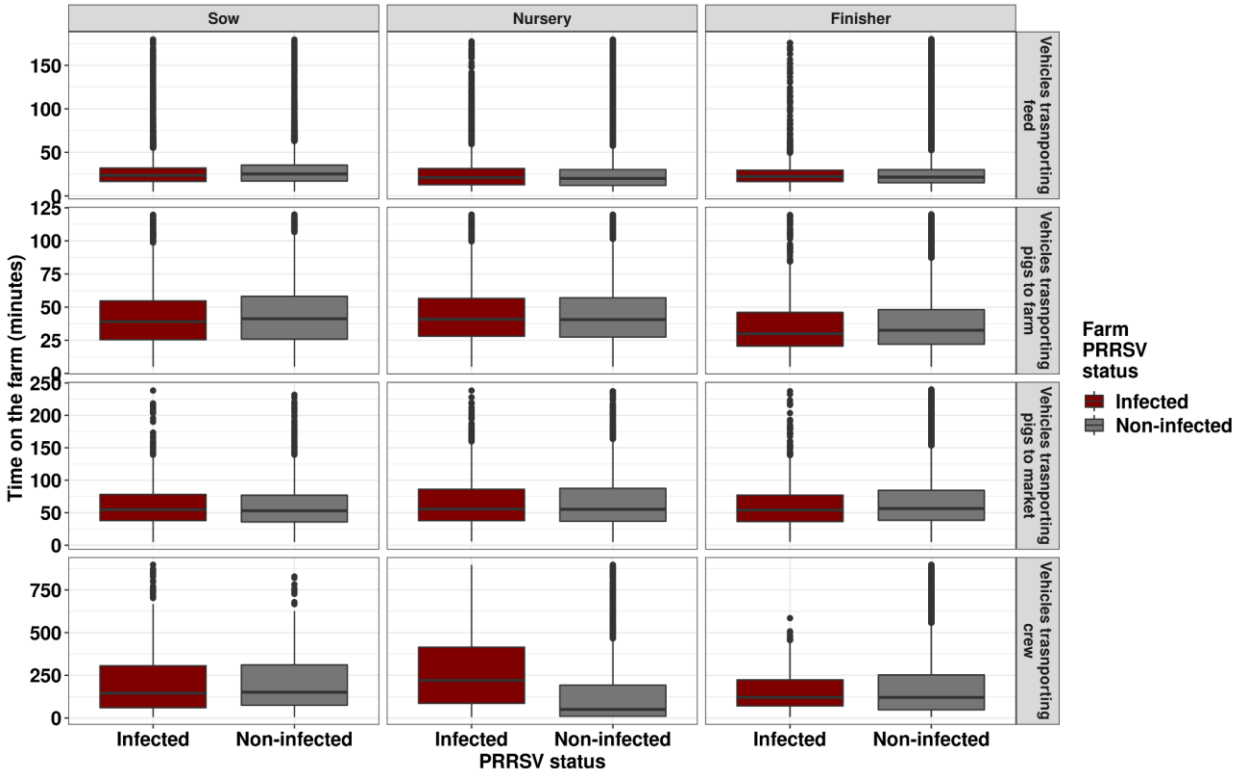

Figure S18. Boxplots compare the time vehicles remain on the farms of infected and non-infected farms for the different transportation vehicles (rows) and production types (columns). Vehicles transporting feed and crew to nursery farms were the only vehicles that showed a higher average of time on infected farms (Mann Whitney test $p < 0.05$).

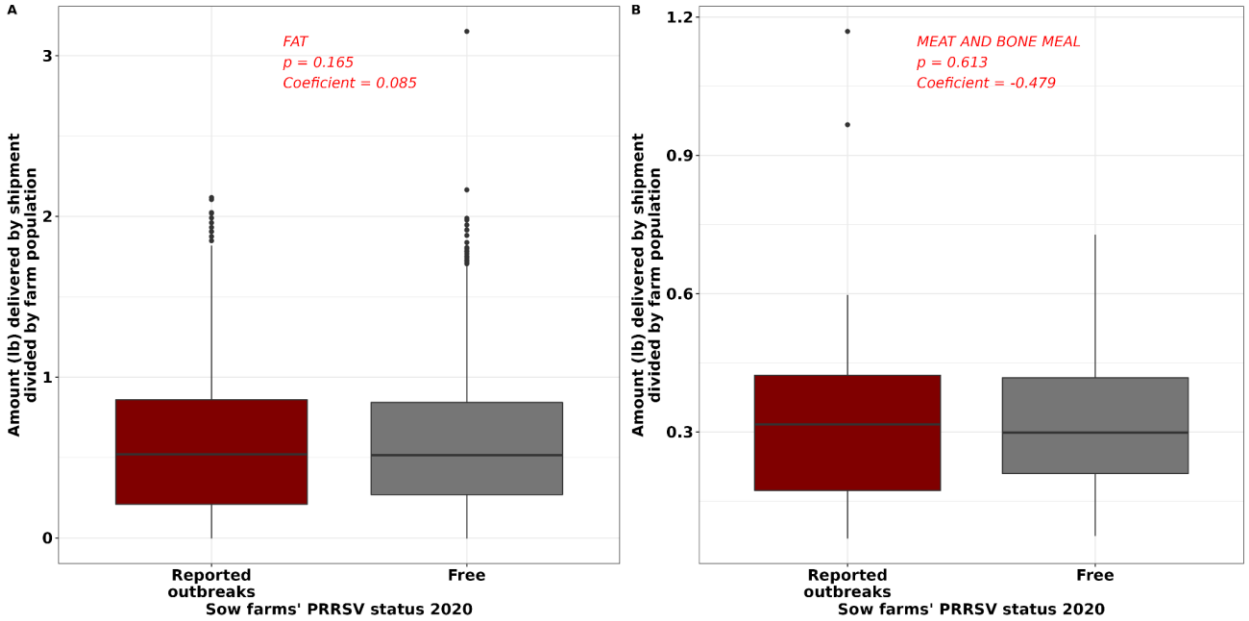

Figure S19. Boxplot comparing the distribution of **A)** fat and **B)** meat and bone in the feed meal received by the sow farms with and without PRRSV records in 2020 (in red the result from the logistic regression).

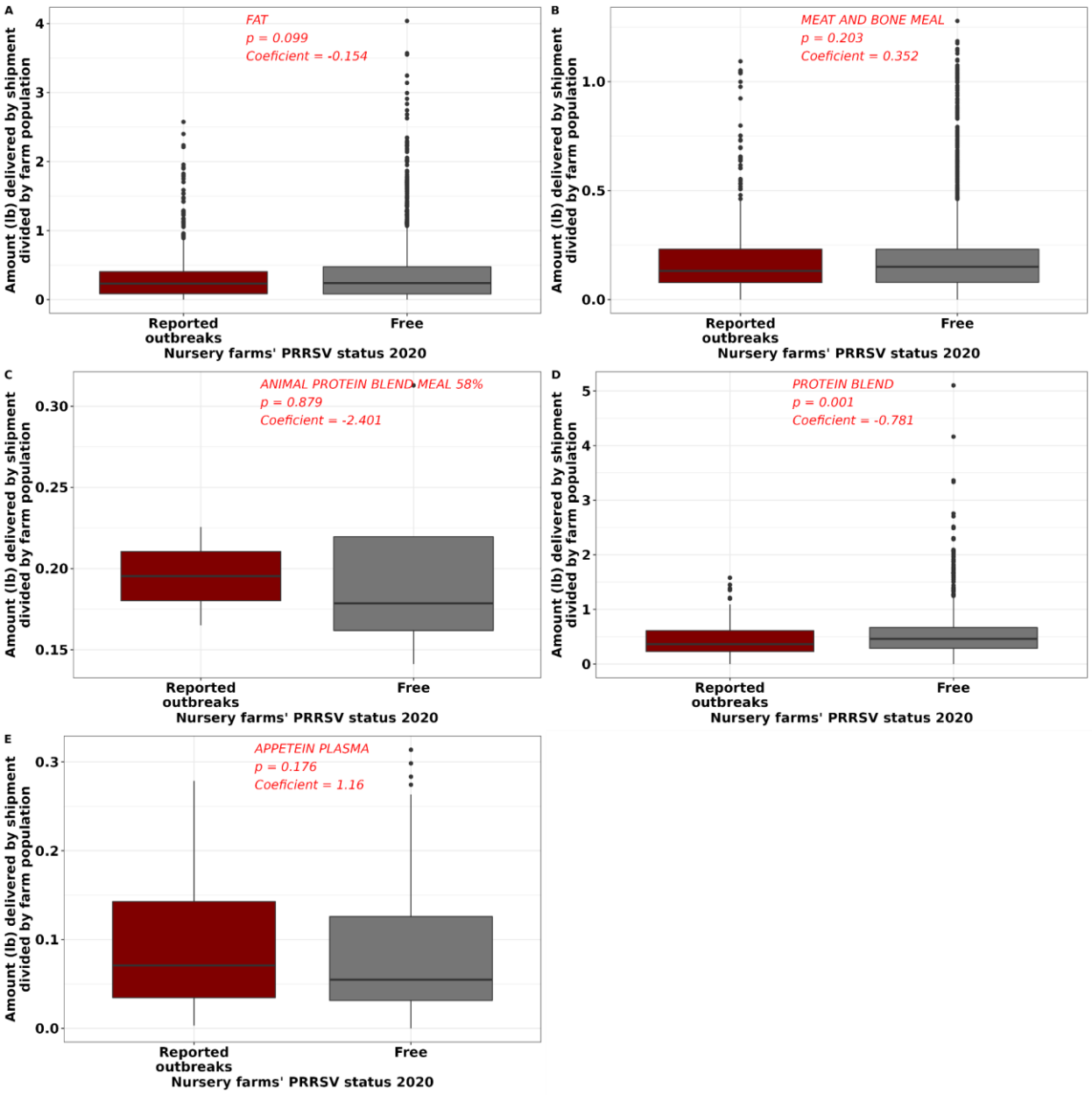

Figure S20. Boxplot comparing the distribution of **A**) fat and **B**) meat and bone in the feed meal received by the nursery farms with and without PRRSV records in 2020 (in red the result from the logistic regression).

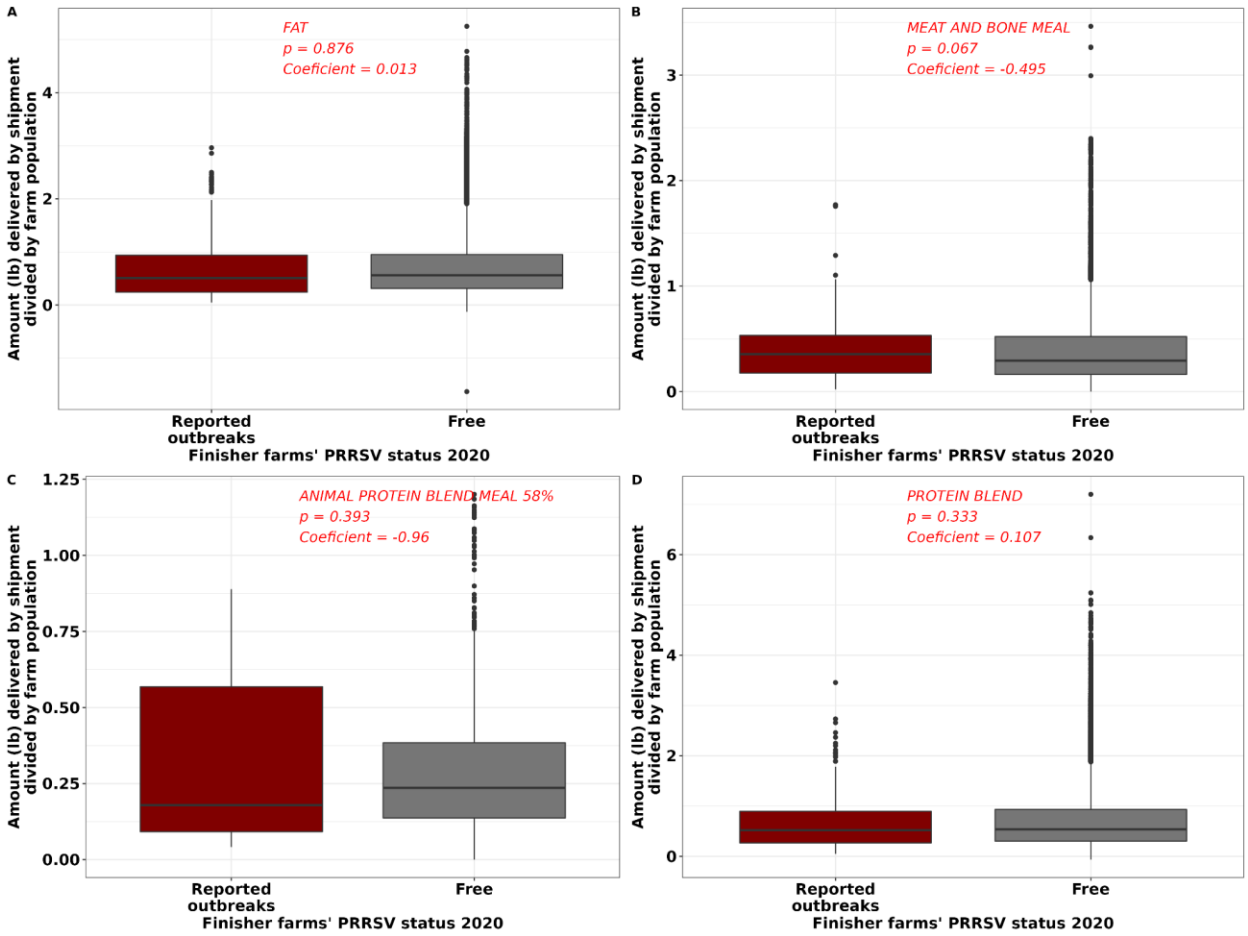

Figure S21. Boxplot comparing the distribution of **A**) fat and **B**) meat and bone in the feed meal received by the sow farms with and without PRRSV records in 2020 (in red the result from the logistic regression).

References

Freeman, L.C., 1978: Centrality in social networks conceptual clarification. *Soc. Netw.* **1**, 215–239, DOI: 10.1016/0378-8733(78)90021-7.

Kao, R.R., D.M. Green, J. Johnson, and I.Z. Kiss, 2007: Disease dynamics over very different time-scales: foot-and-mouth disease and scrapie on the network of livestock movements in the UK. *J. R. Soc. Interface* **4**, 907–916, DOI: 10.1098/rsif.2007.1129.

Lentz, H.H.K., A. Koher, P. Hövel, J. Gethmann, C. Sauter-Louis, T. Selhorst, and F.J. Conraths, 2016: Disease Spread through Animal Movements: A Static and Temporal Network Analysis of Pig

Trade in Germany. (Thierry Boulinier, Ed.)*PLOS ONE* **11**, e0155196, DOI: 10.1371/journal.pone.0155196.

Nöremark, M., and S. Widgren, 2014: EpiContactTrace: an R-package for contact tracing during livestock disease outbreaks and for risk-based surveillance. *BMC Vet. Res.* **10**, 71, DOI: 10.1186/1746-6148-10-71.

Wasserman, S., and K. Faust, 1994: Social Network Analysis: Methods and Applications. Cambridge ; New York: Cambridge University Press.